

Unified analysis of pionic atoms and low-energy pion-nucleus scattering: Phenomenological analysis

R. Seki

*Department of Physics and Astronomy, California State University, Northridge, Northridge, California 91330
and W. K. Kellogg Radiation Laboratory, California Institute of Technology, Pasadena, California 91125*

K. Masutani*

Department of Physics, Faculty of Science, University of Tokyo, Bunkyo-Ku, Tokyo, Japan

(Received 2 August 1982)

The π^- -atom and low-energy π -nucleus elastic scattering data have been analyzed systematically in order to examine their information content with respect to the structure of the π -nucleus optical potential. We have firmly established the existence of the data's insensitivity to the potential structure and have examined its consequences in detail. The insensitivity is manifested in the form of correlations between the coefficients of ρ and ρ^2 in the potential. We have found that such correlations vary slowly as a function of the pion energy (T_π) from the threshold (the π^- atoms) through 50 MeV and that, exploiting the correlations, one can define an effective nuclear density, ρ_e , at which the pion effectively interacts with nuclei. ρ_e was also found to increase slowly as T_π increases. In contrast, no correlation was observed between the coefficient of the local term and that of the nonlocal (momentum dependent) term. As a consequence of the above nature of the correlations, we have established a form of the optical potential which contains the minimum number of parameters in order to describe the information content of the data.

NUCLEAR REACTIONS Unified analysis; strong-interaction shifts and widths in π^- atoms and differential cross sections of elastic π -nucleus scatterings up to 50 MeV; effective nuclear density; π -nucleus optical potentials.

I. INTRODUCTION

Low-energy pions of several tens of MeV have been considered to be a possibly useful probe of nuclei. The major reason for this is that the mean free path of the charged pions (π^\pm) in nuclei is a few fm in this energy region, compared to less than 1 fm in the 3-3 resonance energy region. The positive kaon (K^+) is the only other hadron which has a longer mean free path (of about 7 fm), but the K^+ -neutron scattering amplitude is poorly known and K^+ is not yet as abundantly available as π^\pm . The low-energy pions have the additional advantage that pionic (π^-) atoms can provide information about the π^- -nucleus interaction at the threshold. Such information is supplementary to what we learn from the low-energy scatterings. Numerous, accurate measurements of energy-level shifts and widths in the π^- atoms are available, and the data are described well in terms of the Ericson-Ericson optical potential,¹ which was originally introduced based on multiple scattering theory.

Generally speaking, if one wishes to learn nuclear structure using a hadron, one must know precisely

how the hadron-nucleon scattering amplitude (or interaction) enters the hadron-nucleus optical potential. It is difficult to obtain such reliable information and this has been the major obstacle to nuclear structure study using any hadron. When the hadron-nucleon interaction is weak (that is, the mean free path is long), the optical potential can be approximated by a sum of the hadron-nucleon scattering amplitudes in free space multiplied by the nuclear density. This is the lowest-order approximation in a low-density expansion of the optical potential. Unfortunately, in the case of the low-energy π -nucleus elastic scattering and the π^- atoms, the lowest-order optical potential has been found to be a poor approximation.² The approximation is particularly poor in the local (i.e., momentum independent), scalar part of the potential, where medium corrections are found to be appreciable.

There exists a further complication which is unique to the pion interaction. The major channel in the interaction is an absorption of the pion by a pair of nucleons and results in an optical potential with real (dispersive) and imaginary (absorptive) parts. It is rather difficult even to apply the lowest-

order approximation to these parts because, strictly speaking, the elementary reaction for the process does not exist in free space. The absorption by a deuteron can be useful,¹ but cannot be used rigorously as an elementary process because of the loosely bound structure of the deuteron. In addition, accurate measurements of this process are not yet available in the low-energy region. Therefore, one must resort to constructing the absorption terms from the known π -nucleon amplitudes. It is a difficult task, since the strength of the terms depends directly on the off-energy shell behavior of the amplitudes³ and the initial and final nuclear correlations.⁴ As a convenient approximation the terms are usually expressed as being proportional to $\rho^2 \equiv (\rho_p + \rho_n)^2$. Here ρ_p and ρ_n are the proton and neutron density distributions, respectively. The difficulty of evaluating the absorption terms is manifested in the fact that only recently authors seem to have reached agreement on the sign of $\text{Re}C_0$, the real coefficient of ρ^2 in the momentum dependent part, that it be attractive.⁵ The other parameter, $\text{Re}B_0$, in the momentum independent part, appears to be close to zero,⁵ but there is a conflicting result.³ Actually the pion is absorbed mostly by a pair consisting of the proton and the neutron, but some π^- (π^+) absorption does occur by a pair of protons (neutrons).⁶ A more realistic expression of each absorption term thus requires an additional constant, even if one assumes that the absorption depends only on the isospin of two nucleons, independent of the nuclear species. Clearly, phenomenological determination of ρ_n from data is possible only when such a model is assumed.

One way to circumvent these difficulties is to get help from phenomenology. That is, by temporarily forgetting about obtaining the nuclear structure information and assuming that the potential is expressed as a functional of the conventional ρ_p and ρ_n , one tries to extract information about the functional form by comparing with the π^\pm -scattering and π^- -atom data. This method should work *only if* the data are sensitive to the specific feature of the functional form that is being examined. A comparison to the data of various nuclei could sharpen the sensitivity if the projectile is experiencing the potential somewhat differently for different nuclear targets. Usually what happens is that more than one feature of the potential is sensitive to the data and the sensitivity to one feature can be compensated for by that to the others. Therefore, it becomes a vital question whether the data from various nuclei can provide different information about the potential structure, that is, whether the projectile experiences the potential differently for different nuclear targets. The examination of this question in the low-energy

π -nucleus interactions is an important aspect of this paper.

In the past, the above phenomenological method has been (inappropriately) used in efforts to establish claims that some features of the potential (i.e., corresponding microscopic effects) are significant. What actually has been done is mere illustration of good fits or sensitivity of the parameters describing the particular features to the data, while other parts of the potential are kept fixed, usually to what was considered best at that time. Examples of the features claimed are the Lorentz-Lorenz (Ericson-Ericson) effect (LLE), the π -nucleon finite interaction-range effect, and the nonzero dispersive (real) parts of the absorption terms in the potential. As we pointed out above, these claims are invalid unless one demonstrates that variations due to the uncertainties of the other features are much smaller than the sensitivity of the feature considered. To the best of our knowledge, this demonstration has never been made, and for that matter, no systematic examination has been made of the question as to what and to what extent the low-energy data are really sensitive.

We wish to emphasize that we have studied this question in order to determine to what extent the phenomenology is helpful in the construction of the low-energy pionic optical potential. That is, the purpose of our study was to learn the information content of the elastic pion scattering and pionic atom data regarding the form of the optical potential, but it is *not* a mere numerical exercise in finding another parameter set for the given form of the potential such as the Ericson-Ericson potential.

In our study, we have observed that the information content of the data is far less than we expected from, for example, the numerous, accurate π^- -atom data. Phenomenology is not of much help in the low-energy region, and the above-mentioned claims have been erroneously made, based on the illusory sensitivity that was artificially created by keeping other parameters fixed. In a sense this insensitivity is not a surprising finding; since the pion wavelength is a few fm in this energy region, we should not expect that the pion is sensitive to detailed potential structure, such as a difference between ρ and ρ^2 ($\rho = \rho_n + \rho_p$) dependence which is appreciable only in the surface region over about 0.5 fm.

The insensitivity of the π^- -atom data to the detailed potential structure must have been suspected among workers in the field for some time, though this had never been stated explicitly until recently.⁷⁻¹¹ For example, a frequently quoted relation for the coefficient of ρ^2 , $\text{Re}B_0 = -\text{Im}B_0$, was established¹² as a consequence of a phenomenological

analysis *with the constraint* that the coefficient of ρ , b_0 , is about $0.018\mu^{-1}$ (μ is the pion mass). On the other hand, older phenomenological analyses¹³⁻¹⁵ had given $b_0 \simeq 0.03\mu^{-1}$ with the constraint $\text{Re}B_0 = 0$. A comparison of these analyses clearly suggests a correlation between the two parameters and thus insensitivity of the data. In fact, in the same year that our work on the π^- atoms was reported at a conference,⁷ Tauscher gave an Erice lecture⁹ which included a numerical demonstration of the insensitivity.

After our work described in this paper was completed and most of our results were reported⁷ in conferences, we were informed of an earlier work¹⁶ by a Joint Institute for Nuclear Research Group and of concurrent work^{10,11} by a Michigan State University group. The major aim of the work by these groups was to demonstrate that the pion scatterings can be described well by extrapolating the Ericson-Ericson potential that is fitted to the π^- -atom data. The latter group does report an observation of the insensitivity and an effective nuclear density, but it is a rather fragmented observation. Our study, instead, a systematic, detailed understanding of the insensitivity of the atomic and scattering data. Let us elaborate on this, because our work described in this paper and in the accompanying paper deals with the same topic as that dealt with by the above groups and may be regarded as a report of similar results. In contrast to the work of these groups, we have not aimed at establishing an optical potential which includes various microscopic effects and also describes well the atomic and low-energy scattering data. Such a potential has a structure of great complexity, including many parameters. It is not clear then how much of the potential is verified by experiment or is a consequence of theoretical models. As described above, potential parameters are not well determined microscopically, even within the same model. We wished to establish a potential of the simplest structure containing practically all the information that the atomic and scattering data provide. Parameters in such a potential are therefore effective parameters, and we wished to establish an explicit recipe regarding how one could compare one's potential model against this effective potential. As long as such a recipe is established, it would be a matter of taste whether the potential has an explicit structure of theoretically desirable microscopic effects. As will be discussed in detail in this and in accompanying papers, we have found that the key point of the recipe is the effective nuclear density, which therefore plays the essential role in the low-energy pion interaction. The major objective of our work is thus to establish a clear understanding of this quantity.

After having established the effective potential phenomenologically, we felt that the extrapolation

to low-energy scatterings from the π^- atoms should be examined using this potential so as to clarify what physics is really essential in the unification of two phenomena. We will report on this part of our work in the accompanying paper.

II. INSENSITIVITY OF DATA AND EFFECTIVE NUCLEAR DENSITY

Before we proceed to go over detailed numerical calculations, we wish to clarify the nature of the insensitivity of the data and to discuss the concept of nuclear effective density. The effective density is a consequence of the insensitivity, and these two are the main themes of this paper. Though we specifically deal with the π -nucleus interaction in this paper, the basic ideas are applicable to any hadron scattering.

In order to examine quantitatively the information content of the data with respect to the potential, we must parametrize the potential. The potential form should be general enough to include various features of the pion interaction, but not too complicated so as to get out of hand. The kind of form we chose to examine is expressed in a low-density expansion,

$$V_{\text{opt}} = \sum_{n=0}^{\infty} a_n \rho^n + \sum_{n=0}^{\infty} a'_n \vec{\nabla} \rho^n \cdot \vec{\nabla}, \quad (1)$$

where each a_n and a'_n is a complex, constant parameter whose value depends only on the incident pion energy T_π . Since this form is still too general to handle, in the numerical analysis described in Secs. III and IV we will use two different, more restricted forms of Eq. (1), and generalize the results of the form of Eq. (1). However, discussions in this section will be general enough to be directly applicable to the form of Eq. (1). Throughout the paper we refer the local part of the potential to the first sum on the right-hand side of Eq. (1) (or terms like it) and the nonlocal part to the second sum (or terms like it). The nonlocal form, which stems from the strong π -nucleon p -wave interaction due to the 3-3 resonance, is clearly too restrictive to include highly nonlocal effects. For example, the effect of the finite range in the π -nucleon interaction can be written in a form of Eq. (1), but requires higher-order terms of $\vec{\nabla} \cdot \vec{\nabla}$ as a series expansion. Actually, potentials generally expressed in the form of Eq. (1) have been known to reproduce the experimental data rather well, and as described in the following sections we have also found this to be true. We can thus state that there is no *selective* (unless artificially created, as discussed in Sec. I) significant sensitivity to higher nonlocal effects, and we have decided not to introduce nonlocal terms any more complicated than those in Eq.

(1). Of course, the above observation *does not* mean that higher nonlocal effects are negligible. They may be significant, but the data are just not so sensitive that the form of Eq. (1) could serve as a form of an effective potential. In fact, we have observed that while we can determine the effective strengths to the local and nonlocal parts separately, we cannot determine the individual a_n (or a'_n) unambiguously. The nature of the ambiguity is described by *linear* correlations among a_n 's (or a'_n 's) but not by one between one a_n and one a'_n .

The existence of such correlations associated with the low-energy pion may be expected because of the long wavelength of the pion, as mentioned in Sec. I. Actually, the correlations tend to exist at any energy, though they may not be distinct. We can see this in the following: Consider two Hamiltonians, H and \tilde{H} , which differ by ΔV :

$$H = T + V \text{ and } \tilde{H} = T + V + \Delta V, \quad (2)$$

providing the eigenvalue equations

$$H\psi = E\psi \text{ and } \tilde{H}\tilde{\psi} = (E + \Delta E)\tilde{\psi}. \quad (3)$$

Here T and V denote the kinetic and potential operators, respectively. We then have a relation

$$\Delta E = \langle \psi | \Delta V | \tilde{\psi} \rangle / \langle \psi | \tilde{\psi} \rangle \quad (4)$$

without approximation, where $\langle \psi | \Delta V | \tilde{\psi} \rangle$ denotes $\int \psi \Delta V \tilde{\psi} d\tau$, not $\int \psi^* \Delta V \tilde{\psi} d\tau$, because V and ΔV are complex. Let us assume

$$\Delta V = -\delta a_1 \rho + \delta a_2 \rho^2. \quad (5)$$

Then we have

$$\delta a_2 \langle \tilde{\rho}^2 \rangle = \delta a_1 \langle \tilde{\rho} \rangle + \Delta E, \quad (6)$$

where

$$\langle \tilde{\rho}^n \rangle \equiv \langle \psi | \rho^n | \tilde{\psi} \rangle / \langle \psi | \tilde{\psi} \rangle.$$

Now suppose ΔE corresponds to the uncertainty (times ± 1) associated with a measurement of the binding energy of a system which is described by the Hamiltonian H . If the binding energy is the only information available as $E + \Delta E$, \tilde{H} also describes the system. Actually this \tilde{H} corresponds to the extremes among Hamiltonians which describe the system and are parametrized by δa_1 and δa_2 . That is, Eq. (6) describes a boundary of a region in $\delta a_1 - \delta a_2$ space, and Hamiltonian corresponding to this region yield the same binding energy within the uncertainty. The region is specified by

$$|\delta a_1 \langle \tilde{\rho} \rangle - \delta a_2 \langle \tilde{\rho}^2 \rangle| \leq |\Delta E|.$$

This equation is a nonlinear equation of δa_1 and δa_2 , because $\langle \tilde{\rho} \rangle$ and $\langle \tilde{\rho}^2 \rangle$ depend on δa_1 and δa_2 through $\tilde{\psi}$ that is determined by ΔV of Eq. (5).

Clearly, the size and shape of the region depend on the dynamics (i.e., V) as well as on the magnitude of ΔE . We expect that in some cases the region would be too small to be recognized or even would not exist at all.

Now let us consider the case of our interest, that the region does exist and that $|\Delta E|$ is small compared to $\delta a_2 \langle \tilde{\rho}^2 \rangle$ and $\delta a_1 \langle \tilde{\rho} \rangle$. In this case perturbation theory for V is perhaps applicable, and we write

$$\frac{\delta a_1}{\delta a_2} \simeq \frac{\int \psi \rho^2 \psi d\tau}{\int \psi \rho \psi d\tau} \equiv \frac{\langle \rho^2 \rangle}{\langle \rho \rangle}. \quad (7)$$

Thus we see that when $|\Delta E|$ is "small," the region in the plane which yields E within $|\Delta E|$ tends to be distributed along the linear slope of $\langle \rho^2 \rangle / \langle \rho \rangle$. Therefore we can introduce an effective nuclear density ρ_e defined as $\delta a_1 / \delta a_2$. That is,

$$\langle \rho^2 \rangle = \rho_e \langle \rho \rangle \quad (8a)$$

or

$$\delta a_1 = \rho_e \delta a_2. \quad (8b)$$

ρ_e thus defined is generally a complex number. Actually, in our case we found ρ_e to be approximately real because little interference exists between the real and imaginary parts of the calculation as a consequence of the rather weak π -nucleus interaction. We therefore decided to treat ρ_e as being real by approximating $\langle \rho^n \rangle$ as

$$\begin{aligned} \langle \rho^n \rangle &\equiv \int \psi \rho^n \psi d\tau / \int \psi^2 d\tau \\ &\simeq \int \psi^* \rho^n \psi d\tau / \int |\psi|^2 d\tau \end{aligned} \quad (9)$$

in Eq. (8). This approximation was chosen because of convenience instead of, say, $\langle \rho^n \rangle \simeq \text{Re} \langle \rho^n \rangle$.

The above discussion shows that ρ_e is the correlation parameter for a_1 and a_2 , the coefficients of ρ and ρ^2 . The correlation between them is thus found to be approximately linear, and the correlation parameter ρ_e has the property that an exchange in the potential

$$\rho^2(\vec{r}) \leftrightarrow \rho_e \rho(\vec{r}) \quad (10)$$

effectively yields approximately the same binding energy (or the same scattering amplitude in the case of the continuum, as shown below). Physically, as can be seen in Eq. (10), ρ_e corresponds to the value of the nuclear density at which the pion interacts effectively. However, we note that our definition of the effective nuclear density is not unique. It can be defined differently and thus can have a somewhat different value. For example, we could have defined it as

$$\langle \rho \rangle = \rho_e \langle \theta(R-r) \rangle,$$

where $\theta(x)=1$ for $x \geq 0$ and is otherwise zero. We did not choose this definition because of the awkward nonanalytic property of the uniform nuclear distribution $\theta(R-r)$. But one can see that the introduction of ρ_e is an effort to describe the pionic interaction in finite nuclei (therefore involving the surface) in terms of the interaction in infinite nuclear matter, which is always easier to grasp conceptually. Because of this, some ambiguity is unavoidably inherent in the definition of the effective density. Through this paper and the accompanying one, we define the effective nuclear density as in Eq. (8) with the approximation Eq. (9).

In order to clarify the above general discussion, let us show an example. (The details of the calculations will be given in Sec. III.) Figure 1 shows a $|\Delta E|$ contour for the $1s$ state of the $\pi^- {}^{12}\text{C}$ atom, when the coefficients b_0 (of ρ) and $\text{Re}B_0$ (of ρ^2) in the Ericson-Ericson potential are varied, but the other parameters are kept fixed to the minimum χ^2 values. In the figure there is a minimum. Its dip is shallow, forming a long valley along the direction of about 45° . The length of the valley depends on the choice of $|\Delta E|$; in the present art of measurement $|\Delta E| \approx 0.06 \text{ keV}$.¹⁷ The valley is described by Eq. (6), and from the direction of the valley in the figure we see $\rho_e \approx 1/4\mu^3$ using Eq. (8b).

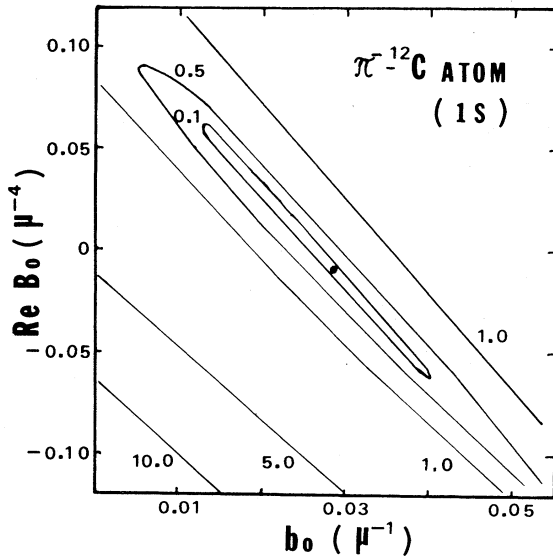


FIG. 1. A sum of the shift and width deviations (added in quadrature) from the best-fit values as a function of the potential parameters b_0 and $\text{Re}B_0$ in the $\pi^- {}^{12}\text{C}$ atom in the $1s$ state. The dot in the middle of the figure corresponds to the best-fit parameter values. The numbers labeling the deviation contours are in keV.

Figure 1 illustrates the correlation between the potential parameters when a single π^- atom is considered. What we really have to consider is a superposition of many such figures for various π^- atoms in various angular momentum states. In Sec. III we will show that most figures have similar valleys in $|\Delta E|$ contours (therefore yielding similar ρ_e 's) and that their superposition yields a valley rather than a well-defined dip (minimum). Therefore, apart from statistics, the correlation appearing in Fig. 1 represents the same general features of the correlation as a consequence of many π^- atom data.

So far we have considered only the case of the π^- atoms. Actually all of the discussion above is also applicable to the case of the low-energy scattering. What we have to do is repeat the identical formalism except that we must replace the eigenenergy E by the scattering amplitudes (times a constant factor)

$$f = \langle \phi_0^{(-)*} | V | \psi^{(+)} \rangle$$

and

$$f + \Delta f = \langle \phi_0^{(-)*} | (V + \Delta V) | \tilde{\psi}^{(+)} \rangle, \quad (11)$$

with the suitable normalization of the wave functions. Here the superscripts $(+)$ and $(-)$ denote the outgoing and incoming waves, respectively, and $\phi_0^{(-)} (= \phi_0)$ is the plane wave. Equation (11) corresponds to Eq. (3) in the π^- atom case. Equation (4) for ΔE is replaced by

$$\Delta f = \langle \psi^{(-)*} | \Delta V | \tilde{\psi}^{(+)} \rangle, \quad (12)$$

which is valid with no approximation. For ΔV given in Eq. (5), we again obtain Eq. (6), in which we have to use the new definition

$$\langle \tilde{\rho}^n \rangle \equiv \langle \psi^{(-)*} | \rho^n | \tilde{\psi}^{(+)} \rangle.$$

The rest of the discussion remains identical, except that the effective density is described as

$$\rho_e \approx \int \psi^{(-)*} \rho^2 \psi^{(+)} d\tau / \int \psi^{(-)*} \rho \psi^{(+)} d\tau$$

rather than by Eq. (8a) with Eq. (9).

Closing this section, we make a pertinent comment. It is known¹⁸ that there exists a group of Hamiltonians which yield the same asymptotic form of the wave functions and therefore the same phase shift and binding energy. The Hamiltonians are related through a unitary transformation called the phase-shift-equivalent (PSE) transformation, which has the property that it must approach unity in the asymptotic region. A question arises as to whether the ambiguity caused by this PSE transformation is the same as the insensitivity that we have discussed in this section. Though our reasoning is not a rigorous proof, we believe that these two have dif-

ferent origins because of the following observation: We have observed that a correlation exists between the ρ and ρ^2 terms in the potential, say, within the local part, but a correlation does not exist between a term in the local part and a counter term in the non-local part. Therefore, if the PSE ambiguity is the same as our insensitivity, the unitary transformation U is such that the PSE potential V_{PSE} ,

$$2\bar{\mu}V_{\text{PSE}} = 2\bar{\mu}U^{-1}V_{\text{opt}}U - [U^{-1}\nabla^2, U],$$

must be momentum-independent (local) even when V_{opt} is local. (Since only the local part of V_{opt} is effective for the π^- atoms in the $1s$ state, this case is not artificial.) Here $\bar{\mu}$ is the reduced pion mass of the system. After some trials using various forms of U , we could not find a U satisfying the above requirement. Even if one could prove such a unitary transformation indeed existed, it would be quite difficult to show that a similar transformation existed also for the nonlocal part: These transformations must not show interference in spite of the fact that the above relation is bilinear in the transformation U . Another reason why we believe that the PSE and the insensitivity are different is that, as seen in Figs. 1, 2, 6, and 8, each χ^2 -contour valley has a finite length and also a minimum, though it is shallow. If the PSE and the insensitivity were the same, the properties of a valley would be independent of the dynamics and it would not show such features.

III. PIONIC ATOMS

V_{opt} of Eq. (1) still has too many terms for a practical numerical calculation. Following the spirit of the low-density expansion, we therefore wished to first examine the leading terms of the expansion, the ρ and ρ^2 terms. Since preferably we can also examine physical effects in such an examination, we decided to choose two forms of the potential for a detailed study. The first one is the Ericson-Ericson potential (EEP) of the form¹

$$(2\bar{\mu}/4\pi)V_{\text{opt}}(\vec{r}) = p_1(b_0\rho + b_1\delta\rho) + p_2B_0\rho^2 - \vec{\nabla}\alpha/(1 - \frac{4}{3}\pi\xi\alpha) \cdot \vec{\nabla}, \quad (13)$$

with

$$\alpha(\vec{r}) = (c_0\rho + c_1\delta\rho)/p_1 + C_0\rho^2/p_2,$$

where

$$\rho \equiv \rho_n(\vec{r}) + \rho_p(\vec{r})$$

and

$$\delta\rho \equiv \rho_n(\vec{r}) - \rho_p(\vec{r}),$$

and

$$p_1 \equiv 1 + \mu/m \text{ and } p_2 \equiv 1 + \mu/2m$$

in terms of the nucleon mass m . The second form is the Kisslinger potential (KIS) (Ref. 19) expressed as

$$(2\bar{\mu}/4\pi)V_{\text{opt}}(\vec{r}) = p_1(b_0\rho + b_1\delta\rho) - p_1^{-1}\vec{\nabla}(c_0\rho + c_1\delta\rho) \cdot \vec{\nabla}. \quad (14)$$

We chose the EEP because it is constructed so as to explicitly describe two-nucleon absorption processes and the Lorentz-Lorenz (Ericson-Ericson) effect. In the EEP the former appears as ρ^2 terms and the latter as nonlinear dependence on $\rho^{1,2}$ in the nonlocal part of the potential. The KIS has no such structure. In the actual calculations the proton and neutron distributions were assumed to be the same (i.e., $\rho_n/N = \rho_p/Z$) and to have the two-parameter Fermi form. In Sec. V we will discuss some possible consequences of removing this restriction from our analysis. When the proton size is folded, the distributions yield the same rms radius $\langle r^2 \rangle^{1/2}$ and $\langle r^4 \rangle^{1/4}$ as those of the charge distributions extracted from high-energy electron scatterings²⁰ and muonic atoms.²¹

The above potentials were put into the Klein-Gordon equation²² as

$$(-\nabla^2 + \bar{\mu}^2 + 2\bar{\mu}V_{\text{opt}})\psi = (E - V_c)^2\psi, \quad (15)$$

Here V_c is the electromagnetic interaction potential. It includes the Coulomb and lowest-order vacuum polarization (Uehling) potentials which are modified by the finite charge distribution of nuclei. Equation (15) was numerically integrated using the computer code MATOM (Ref. 23) to obtain the eigenenergy after the equation was reduced to the standard form of second-order differential equations. The eigenenergy was then corrected for small electromagnetic effects (whenever they were greater than 1 eV) using perturbation theory. These effects consist of the vacuum polarization of $\alpha(Z\alpha)^{3,5,7}$ and $\alpha^2(Z\alpha)$ orders, the static electron-shielding effect, and the center-of-mass motion of the nucleus beyond the reduced mass effect. In this way we accurately computed the binding energy of an atom in a given state once the form of V_{opt} was chosen.

The $|\Delta E|$ contour in the $b_0 - \text{Re}B_0$ plane of Fig. 1 was obtained by repeating the above calculation for various values of the potential parameters b_0 and $\text{Re}B_0$ in the EEP. As discussed in Sec. II, the figure illustrates the correlation between b_0 and $\text{Re}B_0$. We also repeated the calculation by varying the potential parameters c_0 , $\text{Re}C_0$, and ξ (the LLE parameter) in the EEP. A similar correlation was found among these parameters and is illustrated in Fig. 2. Because of the complexity, only the valley is shown for various values of ξ . We observe that when ξ is

varied, the valley slides up and down along almost the same direction as that of the valley itself. We repeated the calculation in other π^- atoms and found that the valleys of the $|\Delta E|$ contours for most of the atoms have practically the same direction in each $b_0 - \text{Re}B_0$ and $c_0 - \text{Re}C_0$ case.

Encouraged with this observation, we proceeded to do best-parameter searches using the EEP and the KIS. We selected 59 pionic atoms in which both shifts and widths had been directly measured^{9,24} after excluding π^- atoms in which more than two, mutually inconsistent data points have been reported. So called upper-width data were also excluded in order to avoid probable prejudice involved in cascade calculations which must be used in the extraction of the data from the x-ray intensity measurements. The π^- atoms of mass number less than 10 were not used in order to avoid complications due to

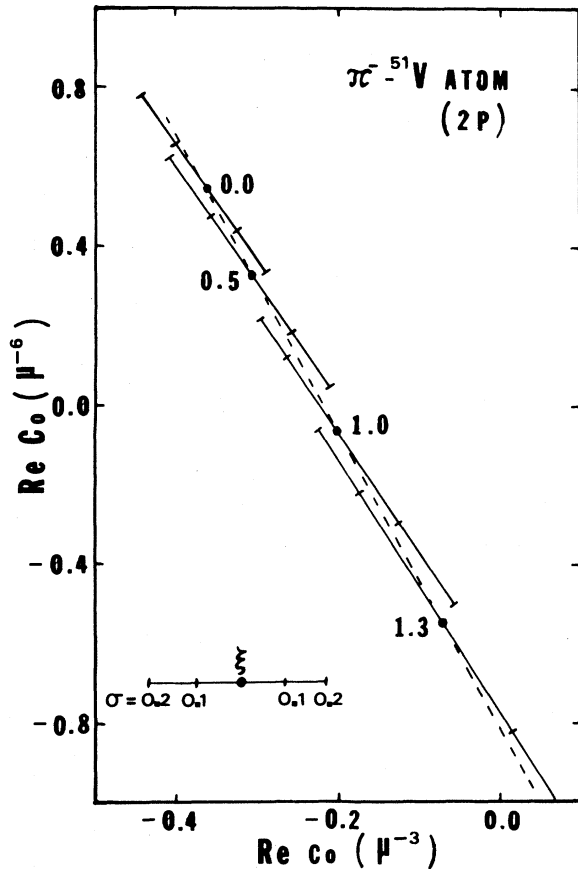


FIG. 2. The same as Fig. 1 in the $\pi^- {}^{51}\text{V}$ atom in the $2p$ state as a function of the Lorentz-Lorenz parameter ξ . For simplicity only the location of the valley is shown for each ξ . The length of the valley is described by the sum of shift and width added in quadrature, σ , expressed in keV.

$1/A$ corrections (A is the atomic mass number).

Table I describes results of the best-fit searches and shows that the EEP and the KIS can be fitted to the 59×2 data with equally good statistics. That is, the data verify neither that the LLE is effective, nor that the two-nucleon absorption process is dominant. This result, as we shall see, seems to be the clearest demonstration of the insensitivity of the π^- atom data to the potential structure. As shown in this table (and also in the following tables) the chi-squares per number of degrees of freedom, χ^2/N , for the best fits are about 3, somewhat large. We will discuss this point shortly.

In order to gain insight, we then repeated the best-fit searches by taking different combinations of the parameters to be fitted. Here, B_0 and C_0 in the EEP were treated to be complex. Table II shows some of the results. Various features can be observed: Once ξ is searched, the uncertainties in c_0 and $\text{Im}C_0$ are increased, as seen in the fit $b-1$ in contrast to the fits $a-1$ and $a-2$. A similar increase in b_0 generated by the search of $\text{Re}B_0$ can be observed in the fits $b-1$ and $b-2$; and though not shown, a similar behavior was also seen in c_0 when $\text{Re}C_0$ was searched for various fixed values of ξ . In fact, when all parameters of interest are searched, little reliable information can be obtained except perhaps for b_0 , b_1 , and $\text{Im}B_0$ as seen in the fit $b-4$. When we compare all searches in the table, we notice a tendency of $\text{Re}B_0 > 0$ and of $\text{Re}C_0 < 0$, but statistically, there is not a conclusive determination of the signs.

Though the parameter values in these tables vary greatly from fit to fit, we observed that there are (linear) relations satisfied by these values. They are

$$\begin{aligned} \beta_s &\equiv b_0 + \alpha_s B_0 \simeq (0.03 - 0.01i) \mu^{-1} \\ &\quad \text{with } \alpha_s \simeq 0.23 \mu^3 \\ \beta_p &\equiv (c_0 + \alpha_p C_0) / \gamma \simeq (-0.2 - 0.02i) \mu^{-3} \\ &\quad \text{with } \alpha_p \simeq 0.37 \mu^3, \end{aligned} \quad (16)$$

where

$$\gamma = 1 - \frac{4\pi}{3} \xi c_0 \rho \simeq 1 - \frac{4\pi}{3} \xi c_0 \rho_e.$$

After examining various analyses of π^- atom data which had been made previously, we find that Eq. (16) is satisfied by parameter values found in the previous analyses.^{9,12-15} (See also the discussion at the end of this section.)

If the unperturbed Coulomb wave function were the correct pionic atom wave function, the r^1 dependence in the region of the nucleus would have provided sensitivity to the details of the potential be-

TABLE I. The best-fit parameters of π -nucleus optical potentials. The numbers in parentheses are kept fixed and not searched. χ^2/N is the chi-square per degree of freedom. μ is the pion mass.

Fit No.	Ericson-Ericson (EEP)		Kisslinger (KIS)	
	$a-1$	$a-2$	$a-3$	
b_0 (μ^{-1})	0.0283 ± 0.0006	0.0283 ± 0.0006	Reb_0	0.0285 ± 0.0006
b_1 (μ^{-1})	0.12 ± 0.01	0.12 ± 0.01	Imb_0	-0.0102 ± 0.0005
ImB_0 (μ^{-4})	-0.042 ± 0.002	-0.043 ± 0.002	Reb_1	0.12 ± 0.01
c_0 (μ^{-3})	-0.223 ± 0.007	-0.176 ± 0.004	Rec_0	-0.173 ± 0.004
c_1 (μ^{-3})	-0.25 ± 0.05	-0.17 ± 0.03	Imc_0	-0.016 ± 0.002
ImC_0 (μ^{-6})	-0.10 ± 0.01	-0.046 ± 0.006	Rec_1	-0.17 ± 0.03
ξ	(1.0)	(0.0)		
χ^2/N	2.9	3.2	χ^2/N	3.0

cause the wave functions of the different π^- atoms in different angular momentum states would have overlapped nuclei in different ways. The insensitivity, therefore, stems from a systematic distortion of the wave functions of the various atoms caused by the strong interaction itself. Figure 3 illustrates this point. The quantity shown is the ratio of expectation values of ρ^2 and ρ , $\langle \rho^2 \rangle / \langle \rho \rangle$, in 59 atoms that were used in the best fit searches. The value of this quantity is equal to $0.24\mu^3$ for most atoms throughout the periodic table both in the case of the EEP and the KIS. This value of $\langle \rho^2 \rangle / \langle \rho \rangle$ is indeed just about equal to the value of α_s in Eq. (16), approximately $0.23\mu^3$. We have thus numerically demonstrated that $\langle \rho^2 \rangle / \langle \rho \rangle$ is the correlation parameter, as suggested in Sec. II. Though not shown, we also observed a similar feature in the case of

$$\langle \nabla \rho^2 \cdot \vec{\nabla} \rangle / \langle \nabla \rho \cdot \vec{\nabla} \rangle$$

for which we obtained $0.38\mu^3$, again numerically close to α_p in Eq. (16). The effective density is thus

$$\rho_e \approx \frac{1}{2}\rho_0 \text{ in the local part,}$$

$$\rho_e \approx \frac{3}{4}\rho_0 \text{ in the nonlocal part,}$$

where $\rho_0 = 0.5\mu^3$ is the nuclear matter density. Note that α and ρ_e differ by a small amount:

$$\alpha_s = (p_2/p_1)\rho_e \text{ for the local part,}$$

$$\alpha_p = (p_1/p_2)\rho_e \text{ for the nonlocal part.}$$

As had been expected, the ratio of two adjacent powers of ρ , $\langle \rho^{n+1} \rangle / \langle \rho^n \rangle$, was found to approach ρ_0 as n becomes large.

Let us examine Fig. 3 in more detail. We observe in the figure that $\langle \rho^2 \rangle / \langle \rho \rangle$ for lighter nuclei in the same angular momentum state is influenced less by

the strong interaction. The value of $\langle \rho^2 \rangle / \langle \rho \rangle$ for light nuclei is smaller than $0.24\mu^3$, and the lighter the nucleus, the smaller the value becomes. It reaches as low as $0.16\mu^3$ for very light nuclei in which generally only the upper-width data are available. In principle, therefore, π^- atom data in these lighter nuclei should provide information about the potential form that is different from the information obtained from the data in medium to heavier nuclei in the same angular momentum state. However, the shift and width data of these lighter nuclei usually carry larger relative errors than those of medium weigh nuclei and therefore weigh less in the best-fit parameter searches. This is particularly true with the presently available upper-width data, and the data serve only as a weak constraint in the searches. In fact, our best fits in Tables I and II reproduced the upper width data with χ^2 per datum less than χ^2/N in the fits. An inclusion of the upper width data in our analysis would not have altered the results significantly.

In the case of heavier nuclei (in the same angular momentum state, of course) we observe that $\langle \rho^2 \rangle / \langle \rho \rangle$ is changed more appreciably by the strong interaction. This means that the stronger potential for heavier nuclei distorts the atomic wave function more than the weaker potential for lighter nuclei does. Consequently, we obtain roughly the same $\langle \rho^2 \rangle / \langle \rho \rangle$ for medium to heavier nuclei and the information content of π^- atom data in these nuclei is basically the same. As exemplified in Fig. 3 for the case of Pd in the $3p$ state, we do not gain much new information about the potential from measurements in very heavy nuclei, such as $E2$ measurements.²⁵ It is rather desirable to obtain more accurate data in light nuclei, i.e., of small shifts and widths and of upper widths.

The fact that $\langle \rho^2 \rangle / \langle \rho \rangle$ has practically the same

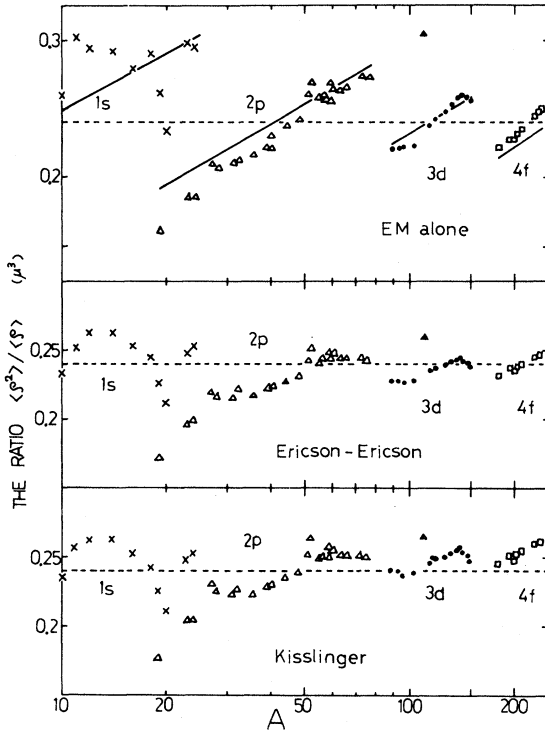


FIG. 3. The ratio of the expectation values, $\langle \rho^2 \rangle / \langle \rho \rangle$ in π^- atoms used in this work. The ratio in each atom is computed by three numerically integrated wave functions: the one without the strong interaction (the top figure) and those with the potential parameters of fits $a-1$ and $a-3$ in Table I (the second and third figures). The ratios for ^{110}Pd in the $3p$ states are shown separately by \blacktriangle . The dotted lines correspond to the ratio of $0.24\mu^{-3}$. Continuous, almost straight curves in the top figure represent the ratios computed by the use of approximated wave functions proportional to r^l , but are being raised by $0.05\mu^3$ for comparison.

value both for the EEP and for the KIS means that the atomic wave functions effectively yield the binding energies independent of the potential forms. This insensitivity of the wave function persists even in the π^- atoms in which the p -state shift changes sign (owing to a dominance of the local part of the potential over the nonlocal part) as A increases. Figure 4 illustrates that the EEP and the KIS predict shifts remarkably close to each other in these π^- atoms once the potentials are fitted to the atoms of lighter nuclei.

In Fig. 5 we plot $\langle \vec{\nabla} \rho \cdot \vec{\nabla} \rangle / \langle \rho \rangle$ for the same set of 59 atoms. We observe that, though values tend to be larger in higher angular momentum states, they decrease for heavier atoms within a given angular momentum state. This feature confirms the property of the π -nucleus interaction, the dominance of the

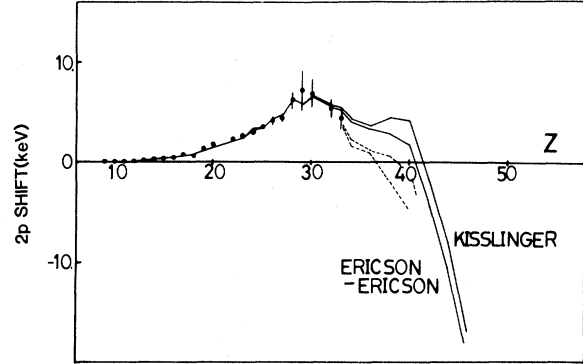


FIG. 4. The $2p$ state strong-interaction shifts in various π^- atoms. The shifts up to the π^- As ($Z=33$) atom are fitted using the potential parameters of fits $a-1$ (EEP) and $a-3$ (KIS) in Table I, and shifts beyond this atom are a prediction. Dotted curves are predicted shifts without the interference from the finite charge distributions of nuclei.

local part over the nonlocal part in heavier nuclei, and is certainly in contrast to what we have observed in Fig. 3 for the quantity $\langle \rho^2 \rangle / \langle \rho \rangle$. We thus conclude that the distortion of the atomic wave functions due to the strong interaction have the following characteristics: The distortions in different atoms appear to be almost the same when viewed through the ρ and ρ^2 terms in the potential, but appear to be different when viewed through the local and nonlocal parts of the potential. As a consequence of this delicate difference, a correlation exists between the coefficients of ρ and ρ^2 but *not* between the parameters of the local and nonlocal parts.

Let us now discuss the problem of the large χ^2/N associated with the best fits. After examining de-

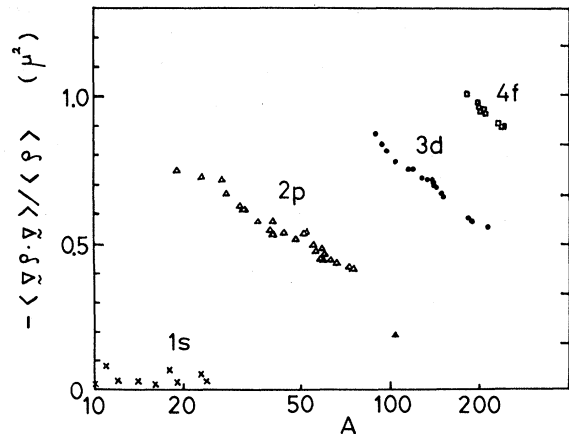


FIG. 5. $-\langle \vec{\nabla} \rho \cdot \vec{\nabla} \rangle / \langle \rho \rangle$ for 59 π^- atoms calculated using the wave functions generated by the KIS potential (fit $a-3$ in Table I).

TABLE II. The best fit parameters of the Ericson-Ericson potentials. The errors in fit $b-4$ are quoted in order to show their size and may not be accurate. The numbers in parentheses are kept fixed and not searched.

Fit No.	$b-1$	$b-2$	$b-3$	$b-4$
b_0 (μ^{-1})	0.0286 ± 0.0006	0.011 ± 0.007	0.012 ± 0.007	0.0208 ± 0.007
b_1 (μ^{-1})	0.12 ± 0.01	0.10 ± 0.01	0.11 ± 0.01	0.09 ± 0.01
$\text{Re}B_0$ (μ^{-4})	(0.)	0.08 ± 0.03	0.08 ± 0.03	0.03 ± 0.03
$\text{Im}B_0$ (μ^{-4})	-0.042 ± 0.002	-0.045 ± 0.003	-0.045 ± 0.003	-0.044 ± 0.003
c_0 (μ^{-3})	-0.22 ± 0.05	(-0.21)	(-0.21)	-0.5 ± 0.4
c_1 (μ^{-3})	-0.25 ± 0.09	(-0.18)	(-0.18)	-1.2 ± 1.1
$\text{Re}C_0$ (μ^{-6})	(0.)	-0.05 ± 0.02	$+0.008 \pm 0.078$	-0.4 ± 2.8
$\text{Im}C_0$ (μ^{-6})	-0.10 ± 0.07	-0.11 ± 0.01	-0.09 ± 0.03	-1.6 ± 3.4
ξ	1.0 ± 0.8	(1.0)	0.7 ± 0.5	4.6 ± 1.5
χ^2/N	3.0	2.8	2.8	3.2

tails of the fits listed in Tables I and II, we found that the widths in ^{18}O and ^{40}Ca atoms and the shifts in F, ^{150}Nd , Th, and U atoms always give large (> 10) χ^2 contributions. When we discarded these data artificially, we obtained smaller values of about 2 for χ^2/N , compared with the original values of about 3. Based on this observation, we had tentatively concluded at the time of the analysis that these data are inconsistent with the rest. It turns out that the ^{18}O , ^{40}Ca , and U data have indeed been revised substantially in the new data discussed below (Ref. 26 for ^{18}O and Ref. 27 for the others).

The degree of the insensitivity does depend on the accuracy of the measurements. After all of the computations described so far were completed, new sets of data were obtained at the Rutherford Laboratory²⁷ and at the Los Alamos Meson Physics Facility²⁸ in some atoms in the $2p$ state and higher. These new data have better accuracy by about an order of magnitude. We have repeated the computations

after replacing some of the old $2p$ state data by the new data from the Rutherford Laboratory in our selected data set of 59 atoms. The results are shown in Table III. The new data give larger χ^2/N of 4.7 for the KIS compared to 3.8 for the EEP. However, because of the largeness of these values and the problem of the isovector parameters as discussed below, we *cannot* conclude that the data are better represented by the EEP than by the KIS.

When we compared the new fits with the old, we noticed that the major change occurred in the isovector parameters (as well as in C_0). Fit $a-3$ in Table I and fit $a-3R$ in Table III tell us that the magnitude of the positive b_1 has increased by about 25% and the magnitude of the negative c_1 has decreased by about 35%. That is, a shift has occurred within the strength of the isovector part of the potential. Let us look into more detail. Using the KIS we write the effective strength of the isovector part as

TABLE III. The best fit parameters for the data including the new $2p$ data (Ref. 27). Blank entries mean that the value is fixed to be zero and is not searched. The numbers in parentheses are kept fixed and not searched.

Fit No.	$a-1R$	$a-3R$	$b-2R$	$b-3R$
$\text{Re}b_0$	0.0285 ± 0.0007	0.0287 ± 0.0008	-0.003 ± 0.008	0.000 ± 0.009
$\text{Im}b_0$		-0.0098 ± 0.005		
b_1	0.14 ± 0.01	0.15 ± 0.01	0.143 ± 0.006	0.11 ± 0.01
$\text{Re}B_0$			0.15 ± 0.04	0.13 ± 0.04
$\text{Im}B_0$	-0.044 ± 0.003		-0.046 ± 0.003	-0.050 ± 0.004
$\text{Re}c_0$	-0.252 ± 0.004	-0.193 ± 0.002	(-0.21)	(-0.21)
$\text{Im}c_0$		-0.013 ± 0.002		
c_1	-0.138 ± 0.05	-0.11 ± 0.03	(-0.18)	(-0.18)
$\text{Re}C_0$			-0.11 ± 0.01	-0.7 ± 0.3
$\text{Im}C_0$	-0.077 ± 0.008		-0.09 ± 0.01	-0.3 ± 0.1
ξ	(1.0)		(1.0)	2.5 ± 0.6
χ^2/N	3.8	4.7	3.5	3.4

$$S_{IV} \equiv b_1 - p_1^{-2} c_1 \langle \vec{\nabla}(\rho_n - \rho_p) \cdot \vec{\nabla} \rangle / \langle \rho_n - \rho_p \rangle \\ = b_1 - p_1^{-2} c_1 \langle \vec{\nabla} \rho \cdot \vec{\nabla} \rangle / \langle \rho \rangle ,$$

where the second equality is a consequence of the restricted model used in our work, $\rho_p/Z = \rho_n/N$. As seen in Fig. 5, $\langle \vec{\nabla} \rho \cdot \vec{\nabla} \rangle / \langle \rho \rangle$ is negative and its magnitude increases from nearly zero to about $1\mu^2$ as the angular momentum of the state increases. Comparing Tables I and III with Fig. 5, we observe that S_{IV} consists of about $0.12\mu^{-1}$ ($=b_1$) and $-0.06\mu^{-1}$ ($=$ the second term) in the case of fit $a-3$ while it consists of about $0.15\mu^{-1}$ ($=b_1$) and $-0.04\mu^{-1}$ ($=$ the second term) in the case of fit $a-3R$. Thus the strength of the isovector part has increased by the inclusion of the new $2p$ data that dominate the best-fit searches. In fact, the analysis accompanying the report of the new data emphasizes the fact that the new data require a larger value of b_1 , $0.13\mu^{-1}$, than the value $0.08\mu^{-1}$ favored by some of the old analyses.

A close examination of fit $a-3R$ shows that a substantial contribution to the χ^2/N now comes from the $1s$ state atoms, compared with fit $a-3$. It is tempting to assert that the new $2p$ data are inconsistent with the old $1s$ data, but the assertion is *not* conclusive because of the ambiguity associated with the determination of the isovector parameters. The ambiguity is caused by the fact that the isovector density distribution $\delta\rho \equiv \rho_n - \rho_p$ is quite sensitive to the choice of the radial dependences of ρ_n and ρ_p . For example, the restricted form $\rho_p/Z = \rho_n/N$ used in our analysis yields $\delta\rho \propto \rho$, but an incompressible nuclear model yields $\delta\rho$ appreciable near the nuclear surface for $N > Z$. Therefore, the values of the isovector parameters, b_1 and c_1 , depend sensitively on the form of $\delta\rho$ used, because the data contain the information of the product of b_1 (or c_1) and $\delta\rho$, but not that of each quantity separately. Our values of the isovector parameters are indeed a consequence of our constraint $\rho_p/Z = \rho_n/N$ imposed at the outset of the analysis, and should not be quoted without this constraint. In the case of the isoscalar param-

eters, the statement is in principle true, but the variation of $\rho \equiv \rho_n + \rho_p$ among various nuclear models is comparatively so small that the values of the isoscalar parameters are approximately the same among different analyses. The values of isovector parameters thus vary among analyses, and their determination requires extra care. We will discuss this problem further in connection with pion scattering at the end of the accompanying paper.

Recently further new atomic data have been reported.^{17,26,29} Unfortunately, in analyses³⁰ which have followed the report of the data, the authors do not use all available data but only selected ones, examining each of some interesting features of the optical potential as a separate analysis. On the other hand, a different group²⁸ has made a serious effort to use the Hartree-Fock nuclear density distributions in the analysis of $2p$ atom data of various isotopes. But again, only selected data among the existing ones are used. Clearly, what should be done is a careful analysis including all available data with the most realistic nuclear distributions available. Until such an analysis is done, it is not clear how much information the presently available data can provide beyond the effective potential. Because of the great amount of effort needed to carry out such an analysis, we have decided to leave it for future work.

IV. PION SCATTERING

Various data have been available for low-energy pion elastic scattering.³¹ Because of convenience and availability, we chose a systematic data set³² of π^+ elastic scattering from various nuclei at $T_\pi = 29.0, 40.0$, and about 50 MeV obtained at the Los Alamos Meson Physics Facility. Based upon the above experience with π^- atoms, we decided to examine the data using just the KIS. In addition, because angular transformation terms³³ (ATT) were known to play an important role in scattering, we also decided to use a modified Kisslinger potential (MKIS). The MKIS has the form π^\pm ,

$$(2\bar{\mu}/4\pi)V_{\text{opt}}^\pm(\vec{r}) = p'_1(b_0\rho \mp b_1\delta\rho) - \{c_0(\vec{\nabla}\rho \cdot \vec{\nabla} - \epsilon\nabla^2\rho) \mp c_1(\vec{\nabla}\delta\rho \cdot \vec{\nabla} - \epsilon\nabla^2\delta\rho)\}/p'_1, \quad (17)$$

where $p'_1 = 1 + 2\epsilon$ and

$$\epsilon = (\mu^2 + k^2)^{1/2}/2m$$

in terms of k , the π -nucleus c.m. momentum. In Eq. (17) the ATT are those with ∇^2 , and without these terms the equation becomes that of the KIS. The KIS for the π^- atoms then has the same form as Eq. (14), except for $p'_1 \neq p_1$, but $p'_1 \rightarrow p_1$ at the threshold.

In the actual analysis we used the same nuclear densities as those used in the π^- -atom analysis (Sec.

III). We then modified the above-mentioned KIS and MKIS by replacing $b_0\rho$ by

$$b_0\rho + (p'_2/p'_1)B_0\rho^2$$

and $c_0\rho$ by

$$c_0\rho + (p'_1/p'_2)C_0\rho^2$$

so as to examine the correlations between the ρ and ρ^2 terms. Here $p'_2 = 1 + \epsilon$. This was done first by numerically integrating the Klein-Gordon equation

using our modified version of a computer code FITPI (Ref. 34) for various values of $\text{Re}b_0 - \text{Re}B_0$ and of $\text{Re}c_0 - \text{Re}C_0$ so as to generate χ^2 contours. We then examined χ^2 contours in each of the $\text{Re}b_0 - \text{Re}B_0$ and $\text{Re}c_0 - \text{Re}C_0$ planes for the existence of the valley. Here we avoided a mere diagonalization of the error matrix near the maximum since we wanted to view the entire valley without the prejudice of linearity. Nevertheless, we have indeed seen a long linear valley in each case and have observed that the direction of the valley varies slowly as the energy increases.

As an example, Fig. 6 illustrates such a valley in the $\text{Re}b_0 - \text{Re}B_0$ plane for the $\pi^+ - {}^{16}\text{O}$ scattering at 49.7 MeV. Choosing three points in the valley, we show in Fig. 7 how the parameters $\text{Re}b_0$ and $\text{Re}B_0$ corresponding to these points reproduce the experimental data. Agreement with the data is of course satisfactory in all three cases, reflecting the fact that the chi-square per number of freedom, χ^2/N , is less than 1.5 for them. We observe, however, an interesting variation in fitting as the parameters $\text{Re}b_0$ and $\text{Re}B_0$ vary from the values corresponding to one end of the valley to those corresponding to the other end, as shown in Fig. 6. A close examination of the Figs. 6 and 7 tells us that appreciable variations occur at the first dip and the shoulder at large angles and confirms an expectation that the accurate measurement at these angles would decrease the amount of the correlation and improve the sensitivity of the data. Note that, when the χ^2 contours in Fig. 6 were obtained in the $\text{Re}b_0 - \text{Re}B_0$ plane, the other parameters were not varied, but kept fixed to the minimum χ^2 values (i.e., corresponding to point *b* in Fig. 6). We also calculated the χ^2 contours by searching the best-fit values for the other parameters

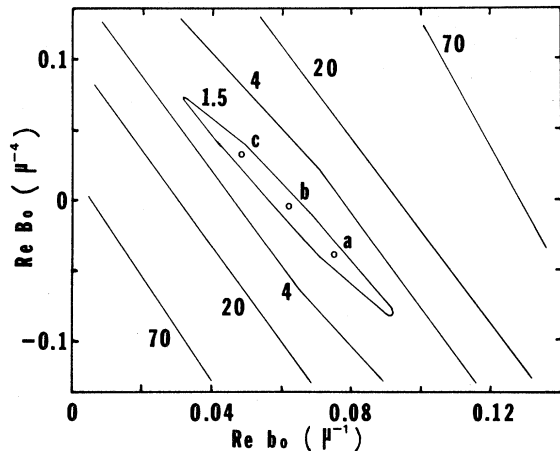


FIG. 6. The χ^2 contours in the $\text{Re}b_0 - \text{Re}B_0$ plane for $\pi^+ - {}^{16}\text{O}$ elastic scattering at 49.7 MeV. Three points *a*, *b*, and *c* in the valley correspond to the curves in Fig. 7.

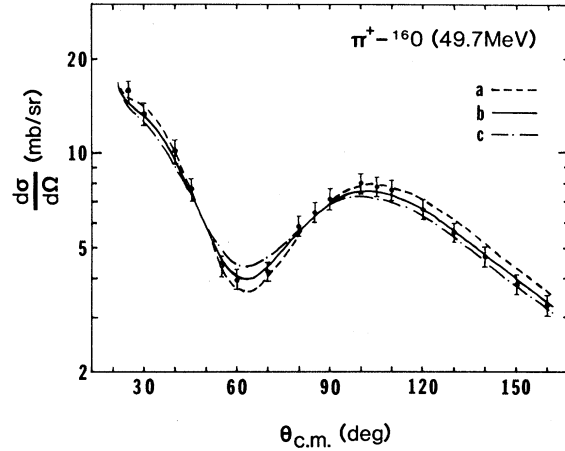


FIG. 7. $\pi^+ - {}^{16}\text{O}$ elastic scattering cross section at 49.7 MeV. The data are from Ref. 31. Three curves labeled *a*, *b*, and *c* correspond to the points in the valleys of the χ^2 contour in Fig. 6.

at each point in the $\text{Re}b_0 - \text{Re}B_0$. In this case the valley was found to be shallower and longer. That is, the insensitivity of the data increased. Figures 6 and 7 thus correspond to the more restricted way of demonstrating the insensitivity of data. We thought, however, that this restricted way more appropriately illustrates our point, and therefore used it for the rest of the analysis.

We repeated the analysis for each nucleus at each energy for the $\text{Re}b_0 - \text{Re}B_0$ and $\text{Re}c_0 - \text{Re}C_0$ planes for the two different potential forms so as to obtain a total of 60 ($=5 \times 3 \times 2 \times 2$) χ^2 contour maps. As an example, Fig. 8 illustrates an intermediate summary of the analysis at 29.0 MeV for the $\text{Re}B_0$ for the KIS by showing the valleys for the various nuclei. Here, the valleys are seen to be indeed linear.

Since all valleys in all χ^2 contour maps turned out to be linear, we decided to describe the valleys using an expression similar to Eq. (16) in the π^- -atom analysis.

$$\begin{aligned} \text{Re}\beta_s &= \text{Re}b_0 + \alpha_s \text{Re}B_0, \\ \text{Re}\beta_p &= \text{Re}c_0 + \alpha_p \text{Re}C_0. \end{aligned} \quad (18)$$

(Note that these equations include the isovector parts, as will be seen below.) Thus α_s , α_p , β_s , and β_p now play the central role in our analysis. We again note that α and ρ_e are different by a small amount:

$$\begin{aligned} \alpha_s &= (p'_2/p'_1)\rho_e \quad \text{for the local part,} \\ \alpha_p &= (p'_1/p'_2)\rho_3 \quad \text{for the nonlocal part.} \end{aligned}$$

Figures 9 and 10 show how the parameters vary for each nucleus at each energy for the two potential forms. These figures represent the final summary of

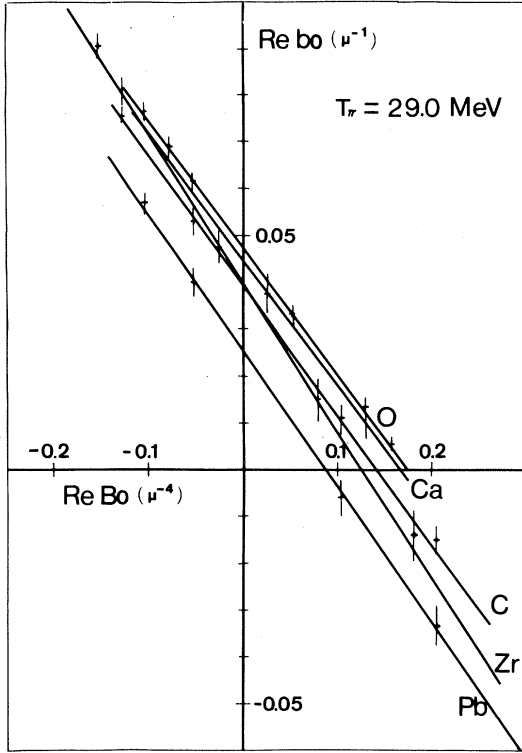


FIG. 8. Valleys of the χ^2 contour in the $\text{Re}b_0 - \text{Re}B_0$ plane at 29.0 MeV. The width of each valley is indicated by error bars which correspond to an increase of χ^2 by the number of degrees of freedom. The range of the valleys that is defined in the same way is shown by the best-fit straight line. Note that the range for Pb exceeds beyond the lower right corner.

our analysis of the low-energy scattering. The figures also include Eq. (16) and a result from the accompanying paper, the threshold values of the α 's and β 's. In Figs. 9 and 10 we observe that, though the values of the α 's (β 's) tend to increase (decrease) in magnitude for heavier nuclei, the values do not scatter too widely among the various nuclei at each energy for each potential form.

As the pion energy increases, the α 's and β 's are seen to increase in magnitude. The values of the α 's for the KIS are slightly (by about 5%) greater than those for the MKIS. The errors in the α 's are difficult to estimate, but we assess them to be in the neighborhood of $0.02\mu^3$, which is comparable to the difference in the values of the α 's for the KIS and MKIS. The energy dependence of the α 's in our energy range (up to 50 MeV) may be taken to be linear (particularly in the case of the MKIS) as a crude but convenient description, even though a slight deviation from the linear dependence seems to appear at 30 MeV. For the MKIS we obtain, by inspection,

$$\begin{aligned}\alpha_s &= 0.22 + 0.0026T_\pi (\mu^3), \\ \alpha_p &= 0.33 + 0.0016T_\pi (\mu^3),\end{aligned}\quad (19)$$

where T_π is expressed in MeV. Strictly speaking, the α 's include those for the $N=Z$ (C, O, and Ca) and $N>Z$ (Zr and Pb) nuclei. We neither know *a priori* how to separate out the isovector components of the α 's nor see a clear pattern of the isospin dependence in Fig. 9. In view of the poor accuracy in the determination of the α 's, further detailed examination does not seem worthwhile at present. In this sense Eq. (19) should be regarded as an expression of the general trend, not as a precise fit.

In the case of the β 's, however, we know that they are the coefficients of the ρ 's in the potential when the KIS and MKIS are regarded as effective potentials. The β 's are then linear sums of the isoscalar and isovector parts, that is, of the effective b_0 (c_0) and b_1 (c_1) at the given energy. We therefore examine the $N=Z$ and $N>Z$ nuclei cases separately in Fig. 10. For the $N=Z$ nuclei, the β 's for the MKIS increase more slowly than for the KIS as the energy increases. In magnitude, the β 's for the KIS are larger than for the MKIS except at the threshold (the π^- atoms) where β_s for the KIS is smaller than for the MKIS. This abnormality turns out to be a reflection of an interesting sign change in the ATT contribution and will be discussed in the accompanying paper. As a convenient summary of Fig. 10 for the $N=Z$ nuclei we again show a linear fit for the MKIS, by inspection:

$$\begin{aligned}b_0(T_\pi) &= \text{Re}\beta_s = 0.031 + 0.00028T_\pi (\mu^{-1}), \\ c_0(T_\pi) &= \text{Re}\beta_p = -0.163 - 0.00060T_\pi (\mu^{-3}),\end{aligned}\quad (20)$$

where T_π is in MeV.

In order to extract the isovector parts as accurately as possible, we averaged the β 's for the $N=Z$ nuclei [i.e., $b_0(T_\pi)$ and $c_0(T_\pi)$] at each energy and then computed $b_1(T_\pi)$ and $c_1(T_\pi)$ from the β 's for the $N>Z$ nuclei. The computation was done using a relation

$$\beta_s = b_0(T_\pi) + \left[\frac{Z-N}{Z+N} \right] b_1(T_\pi)$$

and a similar one for β_p , c_0 , and c_1 , which were obtained exploiting the assumption $\rho_p/Z = \rho_n/N$.

Table IV shows these phenomenological parameter values thus computed. The isovector parameters tend to have smaller magnitudes but the same signs as the pionic atom values. The values for Zr and Pb are unfortunately different, those for Zr being close to zero, but the statistics for these nuclei, particularly for Zr, are not good. The small isovector parameters obtained here will cause some problems when

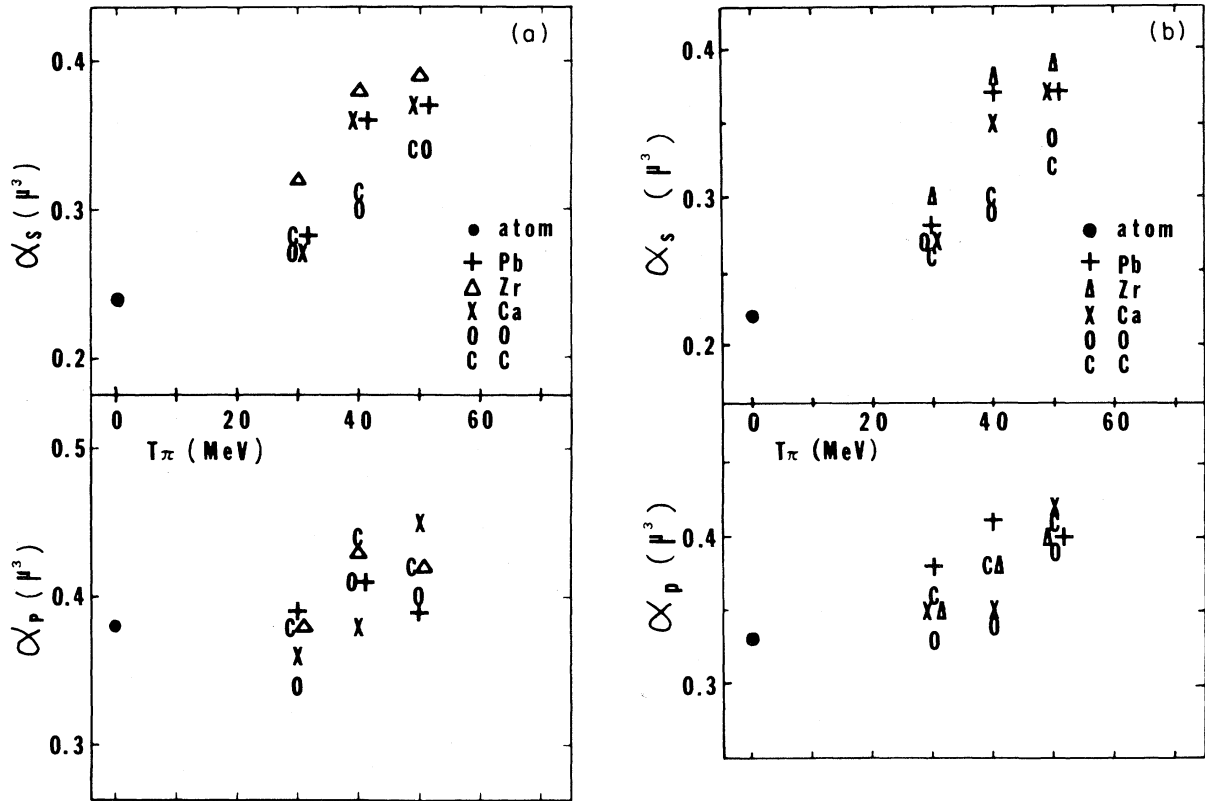


FIG. 9. The energy and atomic-mass number variations of the correlations parameters α_s and α_p obtained using the KIS [part (a)] and the MKIS [part (b)] potentials. C, O, X, Δ , and + denote nuclei of ^{12}C , ^{16}O , ^{40}Ca , ^{90}Zr , and ^{208}Pb , respectively. In part (a) \bullet corresponds to the pionic atom value in Eq. (16) and in part (b) \bullet is also the pionic atom value, but is taken from the analysis in the following paper.

we try to understand the π^- atoms and the scattering in a unified fashion, as described in the accompanying paper.

Closing this section, let us discuss a shortcoming in our analysis of the scattering. The recent elastic differential cross-section data that are used have two types of errors, a relative error and a normalization error. Different values of the former are assigned to different data points, while, for the latter, a single value is usually assigned to all data points for each target of the same experiment. In magnitude the latter is often larger than the former. Since the two types of errors are of different origin, a best-fit parameter search should be done taking into account such a difference. For simplicity, what we did in our analysis was to add in quadrature the two types of errors for each data point and assign the resultant error to each point. Clearly this is an overestimation of the errors. We have, however, examined a few cases, assigning smaller errors by excluding the normalization error, and we have again observed the linear valleys of the χ^2 contour in the ρ - ρ^2 param-

ter planes with practically the same direction for all nuclei at a given energy. The only recognizable feature was that the length and width of a valley were shorter compared to the results we have reported. We therefore believe that what we have reported in this section is correct, though the errors assigned to the results of our analysis may be somewhat overestimated.

V. DISCUSSION AND CONCLUSIONS

Our phenomenological analysis is restricted by the choice of the potential forms of the general type Eq. (1). However, since we did not observe any significant difficulty in fitting potentials to the low-energy data presently available, highly nonlocal effects which depend on large powers of momentum must have been included effectively in the fitted parameter values of our analysis. An example of such effects is the effect due to the finite range of the π -nucleon interaction. A recent, restricted analysis³⁵ concentrating on this effect seems to bear out this

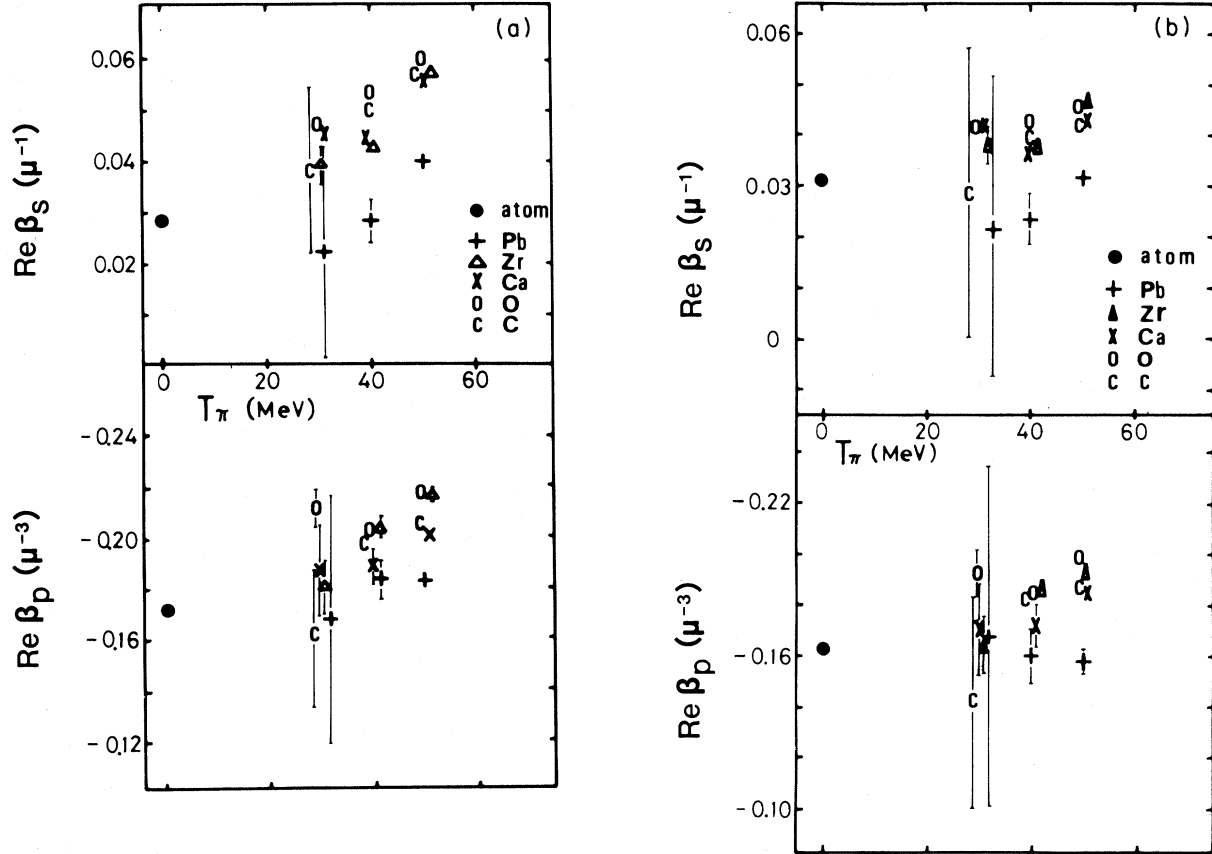


FIG. 10. The energy and atomic-mass number variations of the correlation parameters $\text{Re}\beta_s$ and $\text{Re}\beta_p$ obtained using the KIS [part (a)] and the MKIS [part (b)] potentials. C, O, \times , Δ , and + denote nuclei of ^{12}C , ^{16}O , ^{40}Ca , ^{90}Zr , and ^{208}Pb , respectively. In part (a) \bullet corresponds to the pionic atom value in Eq. (16), and in part (b) \bullet is also the pionic atom value, but taken from the analysis in the following paper.

assertion. At any rate, we have firmly established that there exists an intrinsic insensitivity of the π^- atom and low-energy π -nucleus scattering data to the detailed structure of the optical potential. In this sense good agreement to the data is merely a necessary condition for the soundness of a theory of the optical potential, but not a sufficient one. The

present state of the art does not provide concrete, phenomenological evidence of various microscopic effects such as the Lorentz-Lorenz (Ericson-Ericson) effect and the finite π -nucleon interaction-range effect.

In our analysis we did not consider the effect of uncertainties in the ρ_p and ρ_n . (Actually, what are

TABLE IV. Averaged best-fit isoscalar parameters for C, O, and Ca and deduced isovector parameters for Zr and Pb. The potential form used is the MKIS.

T_π	$\text{Re}b_0$ (μ^{-1})	$\text{Re}b_1$ (μ^{-1})	$\text{Re}c_0$ (μ^{-3})	$\text{Re}c_1$ (μ^{-3})
30 MeV	0.041 ± 0.001		-0.187 ± 0.009	
Zr		0.03 ± 0.04		-0.2 ± 0.1
Pb		0.09 ± 0.14		-0.02 ± 0.30
40 MeV	0.041 ± 0.002		-0.182 ± 0.002	
Zr		0.03 ± 0.02		0.04 ± 0.04
Pb		0.08 ± 0.03		-0.10 ± 0.05
50 MeV	0.045 ± 0.001		-0.192 ± 0.005	
Zr		-0.01 ± 0.01		0.01 ± 0.05
Pb		0.06 ± 0.01		-0.16 ± 0.03

relevant are not just uncertainties in the ρ 's, but those in the proper moments of the ρ 's involved in the π^- atoms and the low-energy scattering.) Even if the restriction $\rho_p/Z = \rho_n/N$ were to be correct, it would still be difficult to assess the influence of uncertainties in ρ_p on the potential-parameter determination. However, as an order-of-magnitude estimate, we may suggest doubling the errors of the isoscalar parameters. The reasons for this suggestion are as follows:

- (1) ρ_p 's for most of the nuclei are determined from μ^- -atom data.
- (2) The corresponding transition energies in π^- and μ^- atoms are similar for a given nucleus.
- (3) The relative uncertainties in energy measurements in these atoms are similar (though generally better in μ^- atoms).
- (4) Therefore the part of the errors caused by the uncertainties in the ρ_p 's is about the same as that caused by the uncertainties in the π^- atoms data. Effectively this argument suggests that we increase the experimental uncertainties in the shift and width data in order to account for the uncertainties in ρ_p 's. When this suggestion is followed rigorously, the errors of the isoscalar parameters should be increased by $\sqrt{2} \simeq 1.4$ rather than doubled. We feel that the overestimate of doubling the errors would be more realistic in view of our restriction $\rho_p/Z = \rho_n/N$.

The influence of this restriction appears directly in the isovector parameters which depend on the form of $\rho_n - \rho_p$. For reasonable choices of individual ρ_n and ρ_p after removing the restriction, the radial dependence of $\rho_n - \rho_p$ varies so greatly that we do not dare make an estimate of the errors in the isovector parameters. These errors are one of the serious problems in π^- atom analyses, and we will discuss this further at the end of the accompanying paper in connection with our hybrid analysis of the low-energy scattering.

Judging from our experience in this work, we feel that, given the present state of the art, a purely phenomenological extraction of the forms of ρ_p and ρ_n is difficult and unreliable and requires much care, particularly in the new sensitivities to various other parameters. This is a general statement. There seems to be,³⁶ however, an exception to this: The low-energy π^- interacts very weakly with the protons. Therefore, if one uses our (effective) KIS or MKIS potential, the π^- differential cross sections depend on two potential parameters, the π^- -neutron parameters in the local and nonlocal parts, as well as on the ρ_n . When a ratio of the π^- cross sections for two isotopes is considered, the ratio then depends effectively only on the single parameter, the ratio of the π^- -neutron parameters, in addition to the ratio of the ρ_n 's for the isotopes. The ratio of the ρ_n 's is

interpreted to correspond to the difference in the neutron rms radius. Thus effectively only two parameters are involved in fitting to the data and they can be determined relatively unambiguously. Note that our ρ_e corresponds roughly to the nuclear density at the rms radius in the case of light nuclei so that the extraction of the rms radius seems to be reasonable. What we have described so far shows why the above technique of extracting the neutron rms radius for two isotopes works, as was demonstrated recently.³⁶ But it also demonstrates how useful it is to apply the concept of the effective nuclear density to low-energy phenomena. We will make an additional comment on the above technique at the end of the accompanying paper.

Concluding this paper, let us summarize the concept of the effective nuclear density: Despite the insensitivity of the data to the detailed potential structure or because of the insensitivity, we found that we can define the effective nuclear density ρ_e . It has the double role of describing the correlation between the ρ and ρ^2 terms in the potential and of defining the approximate region where the π -nucleus interaction is taking place. The value of ρ_e was found to be greater than one-half of the nuclear matter density, to be approximately independent of the atomic mass number of the nuclei, and to increase rather slowly as a function of the pion energy up to 50 MeV.

The concept of ρ_e is perhaps most useful in calculations involving a local density approximation or in nuclear matter calculations. For example, ρ_e represents an approximate nuclear density at which the potential parameters were determined. In this sense, the π^- atom data supply information about the potential at $\rho_e = (\frac{1}{2})\rho_0$ for the local part and at $\rho_e = (\frac{3}{4})\rho_0$ for the nonlocal part. Therefore, it is an extrapolation to apply such a potential to phenomena which involve another region of the nuclear density distribution. For example, our parameters in Eq. (14) and Tables I and II, multiplied by ρ_0 , satisfy the Ericson-Myhrer³⁷ criterion of the existence of a strongly bound state in sufficiently neutron rich nuclei. However, this test does not give us a definite conclusion on the existence of such bound states. [Note that the criterion is not satisfied at $\rho_e = (\frac{3}{4})\rho_0$ even for ³²Na, though this information is not really relevant.]

ACKNOWLEDGMENTS

We acknowledge useful discussions with many colleagues on various occasions over the several years during which this work was carried out. Regarding the initial stage of the work, one of us (R.S.) is indebted to Professor H. Bethe for discussions and suggestions and to Dr. L. Rosen and Dr. J. Brad-

bury for the warm hospitality extended during his sabbatical year (1976–1977) at the Los Alamos Scientific Laboratory (LASL), which is supported by the DOE. The second half of the work was partly carried out at the University of Tokyo. One of us (R.S.) wishes to thank Professor A. Arima and Professor K. Yazaki for the warm hospitality extended during his stay (1977–1978) at the University of Tokyo, where the work was supported in part by the National Science Foundation under Grant No. INT 76-82961. He also expresses his gratitude to Dr. M. Leon and Professor G. Brown for their encouragement and suggestions over the years and also to Pro-

fessor K. Yazaki for various comments after a careful reading of the manuscript. We also wish to thank our colleagues at and associated with LASL, Dr. R. Bauman for supplying us with his group's data before publication and Dr. M. D. Cooper and Professor R. A. Eisenstein for letting us use and modify their code FITPI. This work was supported in part by the DOE under Contract No. DE-AC03-82ER40071 at California State University, Northridge, and by the NSF under Grant No. PHY79-23638 at the California Institute of Technology.

*Present address: SIN, Villigen, CH-5234, Switzerland.

- ¹M. Ericson and T. E. O. Ericson, *Ann. Phys. (N.Y.)* **36**, 323 (1966).
- ²R. H. Landau, in *Proceedings of the 8th International Conference on High Energy Physics and Nuclear Structure, 1979*, edited by D. F. Measday and A. W. Thomas (North-Holland, Amsterdam, 1980), p. 289.
- ³Fr. Hachenberg and H. J. Pirner, *Ann. Phys. (N.Y.)* **112**, 401 (1978).
- ⁴K. Shimizu, A. Faessler, and H. Müther, *Nucl. Phys.* **A343**, 468 (1980).
- ⁵E. Oset, W. Weise, and R. Brockman, *Phys. Lett.* **82B**, 344 (1979); J. Chai and D. O. Riska, *Nucl. Phys.* **A329**, 429 (1979).
- ⁶D. Ashery *et al.*, *Phys. Rev. Lett.* **47**, 895 (1981).
- ⁷R. Seki, contributed paper to the Proceedings of the International Conference on Nuclear Structure, 1977, p. 817; in *Meson-Nuclear Physics—1979 (Houston)*, Proceedings of the 2nd International Topical Conference on Meson-Nuclear Physics, AIP Conf. Proc. No. 54, edited by E. V. Hungerford III (AIP, New York, 1979), p. 616; R. Seki, K. Masutani, M. Oka, and Y. Yazaki, in abstracts of contributed papers, 8th International Conference on High Energy Physics and Nuclear Structure, TRIUMF and the University of British Columbia, 1979, pp. 23,24.
- ⁸R. Seki, K. Masutani, M. Oka, and K. Yazaki, *Phys. Lett.* **97B**, 200 (1980).
- ⁹L. Tauscher, *Exotic Atoms*, edited by G. Fiorentini and G. Torelli (Istituto Nazionale di Fisica Nucleare, Pisa, 1978), p. 145.
- ¹⁰K. Stricker, H. McManus, and J. A. Carr, *Phys. Rev. C* **19**, 929 (1979).
- ¹¹K. Stricker, J. A. Carr, and H. McManus, *Phys. Rev. C* **22**, 2043 (1980).
- ¹²L. Tauscher and W. Schneider, *Z. Phys.* **271**, 409 (1974).
- ¹³M. Krell and T. E. O. Ericson, *Nucl. Phys.* **B11**, 521 (1969). Note that these authors did not optimize the potential parameters.
- ¹⁴D. K. Anderson, D. A. Jenkins, and R. J. Powers, *Phys. Rev.* **188**, 9 (1969); *Phys. Rev. Lett.* **24**, 71 (1970). The first reference uses $\text{Re}B_0 \neq 0$.
- ¹⁵L. Tauscher, *Proceedings of the International Seminar on π -Meson-Nucleus Interactions, Strasbourg, 1971* (Centre National de la Recherche Scientifique, Strasbourg, 1971), p. 45.
- ¹⁶G. G. Bunatyan and Yu. S. Pol', *Yad. Fiz.* **25**, 535 (1977) [*Sov. J. Nucl. Phys.* **25**, 287 (1977)].
- ¹⁷C. A. Fry *et al.*, *Nucl. Phys.* **A375**, 325 (1982).
- ¹⁸B. D. Keister, *Phys. Rev. C* **18**, 1934 (1978), and references therein.
- ¹⁹L. S. Kisslinger, *Phys. Rev.* **98**, 761 (1955).
- ²⁰C. W. deJager, H. de Vries, and C. de Vries, *At. Data Nucl. Data Tables* **14**, 479 (1974).
- ²¹R. Engfer *et al.*, *At. Data Nucl. Data Tables* **14**, 409 (1974).
- ²²H. Feshback and F. Villars, *Rev. Mod. Phys.* **30**, 24 (1958); R. Seki, in *Meson-Nuclear Physics—1976*, (Carnegie-Mellon Conference), Proceedings of the International Topical Conference on Meson-Nuclear Physics, AIP, Conf. Proc. No. 33, edited by P. D. Barnes, R. A. Eisenstein, and L. S. Kisslinger (AIP, New York, 1976), p. 80, and also a preprint, 1982.
- ²³R. Seki (unpublished).
- ²⁴G. Backenstoss, *Annu. Rev. Nucl. Sci.* **20**, 467 (1970).
- ²⁵M. Leon *et al.*, *Phys. Rev. Lett.* **37**, 1135 (1976).
- ²⁶I. Schwanner *et al.*, *Phys. Lett.* **96B**, 268 (1980).
- ²⁷C. J. Batty *et al.*, *Phys. Rev. Lett.* **40**, 931 (1978); *Nucl. Phys.* **A332**, 445 (1979); **A355**, 383 (1981).
- ²⁸R. J. Powers *et al.*, *Nucl. Phys.* **A336**, 475 (1980); K.-C. Wang *et al.*, *Phys. Rev. A* **22**, 1072 (1980).
- ²⁹A. Olin *et al.*, *Nucl. Phys.* **A312**, 361 (1978); **A360**, 426 (1981); C. A. Fry *et al.*, *ibid.* **A375**, 325 (1982); B. H. Olaniyi *et al.*, *ibid.* **A384**, 345 (1982).
- ³⁰E. Friedman and A. Gal, *Nucl. Phys.* **A345**, 457 (1980); Y. Alexander, A. Gal, V. B. Mandelzweig, and E. Friedman, *ibid.* **A356**, 307 (1981); E. Friedman, *Phys. Lett.* **104B**, 357 (1981).
- ³¹References in R. H. Landau, *Proceedings of the 8th International Conference on High Energy Physics and Nuclear Structure*, edited by D. F. Measday and A. W.

- Thomas (North-Holland, Amsterdam, 1980), p. 289; C. H. Q. Ingram, Nucl. Phys. A374, 319c (1982).
- ³²B. M. Freedom *et al.*, Phys. Rev. C 23, 1134 (1981); M. Blecher *et al.*, *ibid.* 20, 1884 (1979), and references therein.
- ³³M. Theis, Phys. Lett. 63B, 43 (1976) and references therein; G. A. Miller, Phys. Rev. C 10, 1242 (1974), and references therein.
- ³⁴M. D. Cooper and R. A. Eisenstein (unpublished).
- ³⁵Y. Alexander *et al.*, see Ref. 30.
- ³⁶A. W. Thomas, Nucl. Phys. A354, 51 (1981).
- ³⁷T. E. O. Ericson and F. Myhrer, Phys. Lett. 74B, 163 (1978).